International Conference on Mathematics, Computational Methods & Reactor Physics (M&C 2009)
Saratoga Springs, New York, May 3-7, 2009, on CD-ROM, American Nuclear Society, LaGrange Park, IL (2009)

A LINEAR-DISCONTINUOUS CUT-CELL DISCRETIZATION FOR THE S_N EQUATIONS IN R-Z GEOMETRY

Michael S. Reed[*] and Jim E. Morel
Department of Nuclear Engineering
Texas A&M University
College Station Texas
reedms@nv.doe.gov; morel@tamu.edu

ABSTRACT

We have developed, implemented, and tested a new linear-discontinuous Galerkin cut-cell discretization for the S_n equations in R-Z geometry. This approach represents an alternative to homogenization in rectangular spatial cells containing a material discontinuity (referred to as mixed cells). A line is used to represent the boundary between the two materials in a mixed cell converting a rectangular mixed cell into two non-orthogonal, homogeneous sub-cells. The linear-discontinuous Galerkin spatial discretization is used on all of the rectangular cells as well as the non-orthogonal sub-cells. The method is described and computational results are presented that demonstrate second-order accuracy in multi-material problems with curved material interfaces. Additionally some evidence is provided that indicates that the cut-cell method is more computationally efficient than employing homogenization.

Key Words: discontinuous-Galerkin, cut-cells, discrete-ordinates

1. INTRODUCTION

The purpose of this summary is to describe a new linear-discontinuous Galerkin cut-cell discretization for the S_n equations in R-Z geometry. Cut-cell methods are commonly used in computational fluid dynamics [1] but have found little application in radiation transport. Our approach represents an alternative to homogenization in rectangular spatial cells containing a material discontinuity (referred to as mixed cells). A line is used to represent the boundary between the two materials in a mixed cell converting a rectangular mixed cell into two non-orthogonal, homogeneous sub-cells. A single cut-cell is illustrated in Fig. 1. The linear-discontinuous Galerkin spatial discretization is used on all of the rectangular cells as well as the non-orthogonal sub-cells. There are three main advantages to our approach relative to the use of unstructured meshes. First, a linear representation for an interface between materials offers the potential for second-order accuracy even when the interface is curved. Second, the significant advantages for parallel computation on rectangular meshes relative to unstructured meshes are retained for a cut-cell mesh. Third, cut-cell meshes are far easier to generate than general unstructured meshes. One could obviously treat multiple material interfaces within a single cell

[*] Present address: Remote Sensing Laboratory Las Vegas, NV.

using the cut-cell approach, but we restrict ourselves in this study to two-material interfaces since this suffices to demonstrate the efficacy of the approach.

The remainder of this summary is organized as follows. First we describe the basic equations associated with our method and the details of its implementation. Then we present computational results comparing our approach with homogenization. Finally, we present conclusions regarding the efficacy of our method.

2. THE CUT-CELL METHOD

Fig. 1 depicts a rough representation of a fuel pin cell arising in the modeling of nuclear reactors. We note that any orthogonal meshing of this geometry results in cells that contain material interfaces. This is an example of where interface reconstruction is needed. We proceed by considering how such a pin cell would be handled by our new method.

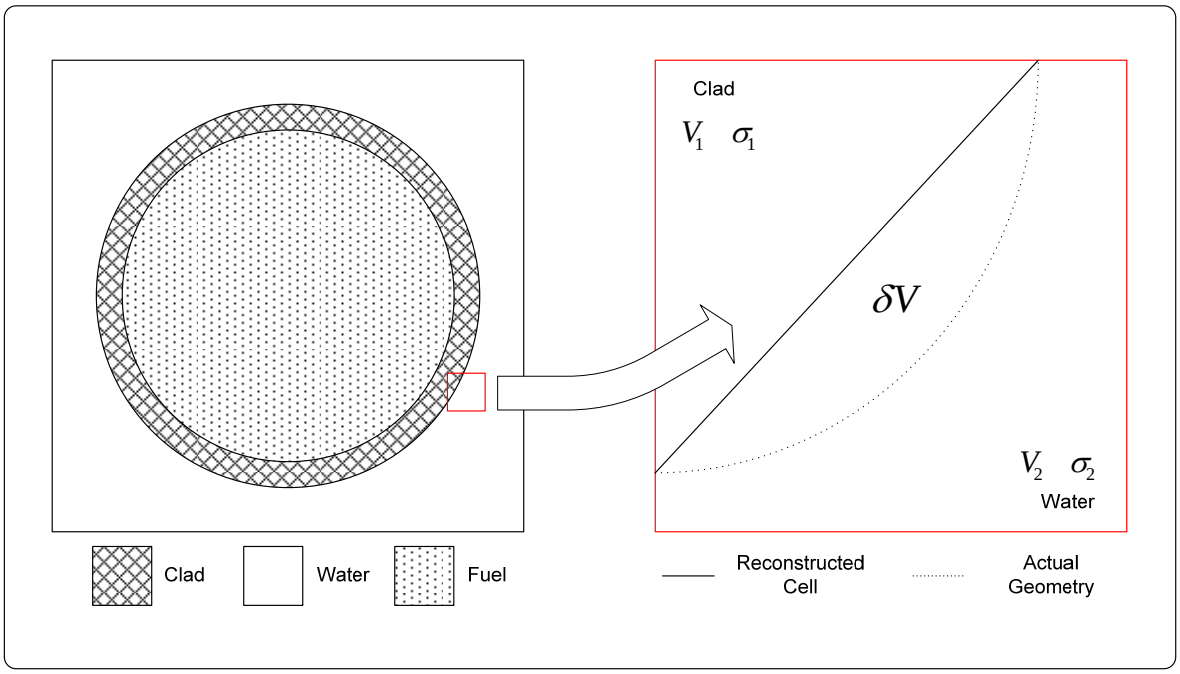

Figure 1. Typical Cut-Cell Depiction

2.1. Mesh Generation

Our cut-cell method begins by meshing the pin cell with a rectangular grid with no attention paid to the presence of material interfaces. This base grid is then further subdivided into cut-cells in regions where a material interface passes through the base grid. The material interfaces are then represented as linear segments within each cut-cell. This approach results in the classical rectangular mesh with a small number of cells having substructure defined by the union of two smaller polygons. For this work we restrict ourselves to a single level of subdivision. Such a

restriction results in cut-cells composed of a combination of quadrilaterals, triangles, and pentagons.

The diagram in Fig. 1 shows the resulting substructure that arises from representing a curved material interface by a linear segment. The linear segment is located so that it coincides with the actual material interface at two points. These two points are located where the actual interface intersects the faces of the mixed cell. There are obviously other ways to locate the segment, but we judged this approach to be the least problematic. We make note of the sliver of volume δV lying between the true interface and the linear representation.

2.2. Sliver Treatment

The inability of the linear mesh to conform to curvilinear boundaries results in the presence of cutcells whose underlying polygonal elements are not truly homogenous. Typically, one of the polygonal sub-cells will be homogenous and the other will not be. There exist at least 3 reasonable ways to handle this. The traditional approach used in fluid dynamics applications is to preserve the total mass of each material contained in a cut-cell. For particle transport this results in modification of the macroscopic cross sections in each sub-cell. This cell-wise approach is fairly accurate but is noisy. A less noisy approach is to modify the density within each homogeneous material region to preserve the total mass in that region. This approach is much smoother because the relative change required in the mass of a region is much smaller than the relative change in the masses of individual sub-cells. One more approach to handling the sliver volume is to simply ignore the sliver and accept the associated meshing error. With increasing spatial refinement the associated meshing error is reduced.

Our experience indicates that the finite element treatment itself determines the order of convergence of a method, while the sliver treatment merely affects accuracy. Although not universally most accurate, a region-wise mass preservation treatment is quite accurate and not subject to the degree of noisiness seen in a cell-wise mass preservation approach.

2.3. Numerical Discretization

The linear-discontinuous Galerkin S_n equations with weighted diamond angular discretization [2] may be written for a weighted direction on an arbitrary polygon as:

$$\sum_{\substack{s=1,\\ \underline{n}_s\bullet\underline{\Omega}_m>0}}^{S} \int_{L_s} dL_s\, b_i \left|\underline{n}_s\bullet\underline{\Omega}_m\right| r\psi_m \;-\int_{A_{cell}} dA\, r\psi_m\, \underline{\Omega}_m\bullet\underline{\nabla} b_i + \int_{A_{cell}} dA b_i\, r\sigma\psi_m - \int_{A_{cell}} dA b_i\, \beta_m \psi_m$$
$$= \sum_{\substack{s=1,\\ \underline{n}_s\bullet\underline{\Omega}_m<0}}^{S} \int_{L_s} dL_s\, b_i \left|\underline{n}_s\bullet\underline{\Omega}_m\right| r\psi_m + \int_{A_{cell}} r\, b_i\, Q_m dA - \int_{A_{cell}} dA\gamma_m\, b_i\, \psi_{m-1/2} \quad . \tag{1}$$

Here the angular index is denoted by m, and the inflow angular edge index is $m-1/2$. The angular flux of particles associated with direction m is denoted by ψ_m. The direction of particle flight is denoted by the unit vector $\underline{\Omega}_m$ and the sides of the arbitrary polygon are denoted by $s=\{1\ldots S\}$ with corresponding outward unit normals $\underline{n}_s$. The basis functions are denoted

by $b_i = \{b_0, b_r, b_z\}$, the total cross section is denoted by σ, the total source term is denoted by Q_m, and the terms β_m and γ_m are angular differencing coefficients.

The spatial leakage terms are separated on each side of the equation with the inflow fluxes coming from the upstream closure. The angular flux as a function of the spatial variables r and z is expanded as a combination of basis functions and unknown coefficients:

$$\psi_m(r,z) = b_0(r,z)\psi_m^0 + b_r(r,z)\psi_m^r + b_z(r,z)\psi_m^z \ . \tag{2}$$

By substituting this linear expansion for the angular flux into Eq. (1) one obtains a 3x3 matrix equation on a polygon. This equation may be solved for the unknown angular flux coefficients given upstream spatial inflow fluxes and an angular inflow flux. We solve the starting direction flux equations to obtain the initial angular inflow fluxes on each angular quadrature level. This space-angle discretization is used for all the cells associated with our cut-cell method.

3. COMPUTATIONAL RESULTS

In order to investigate our cut-cell method we generate the required cut-cell meshes by modeling 1-D spherical geometry using a 2-D RZ mesh. This approach allows us to run spherical shells that generate cut-cell meshes at the annuli boundaries. We present results for both a manufactured solution and a k-eigenvalue problem.

3.1. Manufactured Solution Test Problem

In order to verify the correctness of our implementation as well as evaluate the performance of our method, we use the method of manufactured solutions. Manufactured solutions start with an arbitrary solution to the transport equation that may be tailored to suit particular purposes. This solution is then substituted into the transport equation to find the inhomogenous source giving rise to that solution. The result is then used as input to a transport code. The known solution may then be compared against that obtained by the numerical method. In this way the accuracy and order of convergence of the method may be determined.

For our purposes we consider a 1-D spherical manufactured solution containing two spatial kinks (discontinuities in the spatial derivative) in the angular flux that simulate the effect of a material discontinuity. We choose an angular flux that is piecewise defined on a spherical domain with one linear component and one quadratic component. The angular flux for this manufactured solution in terms of the spherical spatial variable x is:

$$\psi = \begin{cases} x^2 & , \quad x \in [0, x_A] \ , \\ \dfrac{x_A^2}{x_A - x_B}(x - x_B) & , \quad x \in [x_A, x_B] \ , \\ 0 & , \quad else \ . \end{cases} \tag{3}$$

We note that this solution satisfies the 2-D RZ boundary condition along the z-axis as well as vacuum boundary conditions. For this test problem we generate the source for this manufactured solution using a uniform, purely absorbing medium of $\sigma = 1 cm^{-1}$ with dimensions $x_A = 0.5 cm$ and $x_B = 1.0 cm$.

The presence of curved spatial kinks in the solution is problematic for quadrature evaluation of the inner products appearing in Eq. (1). Nonetheless we choose to employ standard spatial quadratures to evaluate them. More specifically, a standard 9-point Gaussian quadrature set is used on quadrilaterals, and a standard 4-point set is used on triangles. All pentagonal elements are integrated via decomposition into triangles. While the use of standard quadratures introduces a slight amount of noise in the solution for this particular problem, our computational results indicate that they are sufficiently accurate.

We use this manufactured solution to evaluate the convergence rate of the scalar flux for this test problem. For this problem we use the S_4 Gauss-Chebyshev triangular quadrature set in angle and make no accounting for the volume sliver. Figure 2 gives the rate of convergence of a cell-wise evaluated L_2 norm of the S_n scalar flux for this manufactured solution. It can be seen from Fig. 2

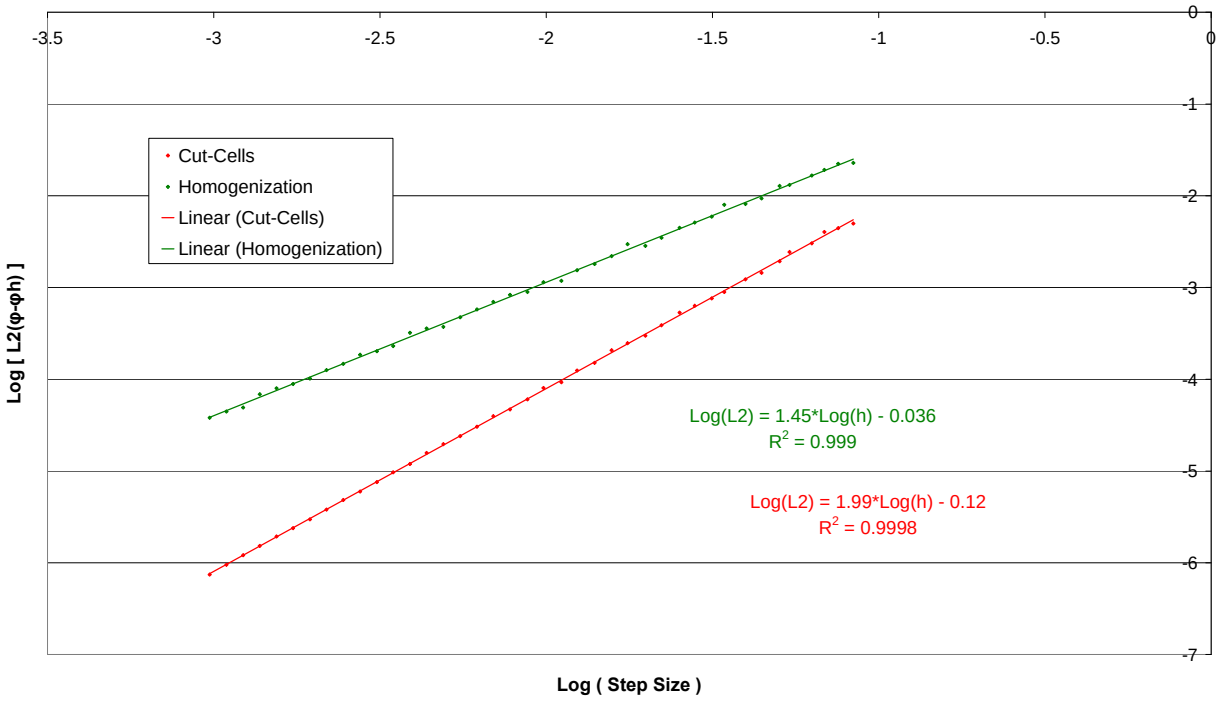

Figure 2. Scalar Flux Convergence in Spherical Manufactured Solution

that one obtains second-order convergence for the L_2 norm of the scalar flux using the cut-cell method. In comparison, the effect of homogenizing the mesh results in an order of convergence of approximately 1.5. In addition, the cut-cell method is significantly more accurate for a given mesh size. Considering the coarsest mesh shown in Fig. 2, one may see that even when viewed on the basis of total unknowns, the cut-cell method yields an error approximately 4.5 times lower than that given by a homogenized mesh containing the same number of unknowns. Although we

show results for only a single problem here, our experience has shown the cut-cell method to be universally more accurate for all problems considered.

3.2. Eigenvalue Test Problem Convergence

Our new cut-cell method was also tested on a k-eigenvalue calculation consisting of a spherical fuel region surrounded by a spherical shell moderator region. The fuel region has thickness $t^{fuel} = 0.25\,cm$, and has material properties $\sigma_t^{fuel} = 1 cm^{-1}$, $\sigma_s^{fuel} = 0.1 cm^{-1}$, and $\nu\sigma_f^{fuel} = 1.0\,cm^{-1}$. The moderator region has thickness $t^{mod} = 0.25\,cm$, and has material properties $\sigma_t^{mod} = 2\,cm^{-1}$ and $\sigma_s^{mod} = 0.8\,cm^{-1}$. This system is modeled using 2-D cylindrical geometry that results in the cut-cell treatment at the fuel/moderator interface as well as at the moderator/vacuum interface. For this test problem we use the S_4 Gauss-Chebyshev triangular quadrature set in angle and employ a region-wise mass preservation technique. The convergence of the eigenvalue is calculated using a solution obtained on a very fine spatial mesh using the same angular quadrature set. The results of the eigenvalue study are depicted in Figure 3.

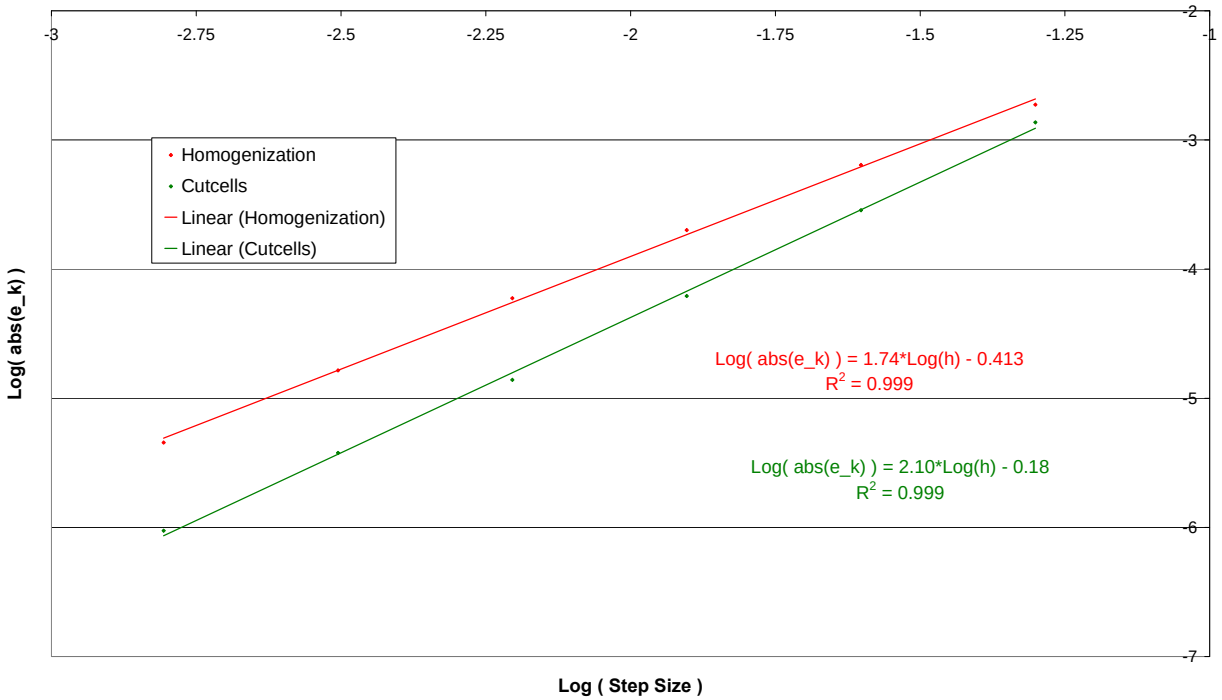

Figure 3. Convergence of Eigenvalue in Spherical Test Problem

This figure indicates that the cut-cell method is second-order convergent for the eigenvalue. The actual slope of the trend is slightly larger than 2 because the results are plotted against the mesh size for the orthogonal base grid. In comparison, homogenization has an effective order of convergence of approximately 1.75. The global nature of the eigenvalue as well as the location of the interface explains a slightly better order of convergence for homogenization as compared to

the scalar flux convergence for the manufactured solution. The cut-cell method is again significantly more accurate than homogenization. Calculations depicted in Figure 3 for the two finest meshes correspond to base orthogonal grids of 160x320 and 320x640 cells. We note that the cut-cell method yields a more accurate result on the 160x320 grid than does homogenization on the 320x640 grid.

3.2. Eigenvalue Test Problem Computational Efficiency

Though we make no attempt at a rigorous cost analysis for the cut-cell method, we present a rough comparison of the cut-cell method with homogenization on the basis of computation time required to achieve a solution to a given precision. To this end we obtain solutions to the eigenvalue problem on several meshes. We also tally the processor time required to obtain those solutions. For this work both methods were implemented using a 3.0 ghz Intel Wolfdale processor with 8gb of memory. The code itself is single-threaded and written in Fortran 90 compiled using the default speed optimized profile on the Intel Fortran 10.1 compiler. The timing is taken from the processor clock itself and is measured from the start of meshing to the point at which convergence criteria on the scalar fluxes and eigenvalue is obtained. The results are compiled in Table I.

Table I. Eigenvalue Test Problem Processor Time

		Homogenization		Cut-Cells	
Base Grid	Number of Cutcells	Abs(e_k)	Time (sec)	Abs(e_k)	Time (sec)
10x20	40	9.71E-03	0.36	2.75E-03	0.56
20x40	76	1.87E-03	1.08	1.37E-03	1.42
40x80	156	6.39E-04	4.56	2.86E-04	5.16
80x160	316	2.00E-04	18.45	6.17E-05	20.55
160x320	636	5.94E-05	79.51	1.39E-05	80.11
320x640	1276	1.64E-05	332.64	3.77E-06	339.89
640x1280	2556	4.53E-06	1444.24	9.43E-07	1435.68

For the eigenvalue test problem that is considered, the cut-cell method is more computationally efficient on all but the coarsest of meshes. At the fundamental level the cut-cell method incurs additional computational cost to set up data structures for sweeping on non-orthogonal grids as well as the additional cost incurred in performing integrations on general polygons. However, the inability of homogenization to accurately represent discontinuities in cross sections and corresponding kinks in the angular flux solution severely limits its accuracy. Because of the nature of the spherical shells being modeled, the resulting number of cut-cells scales linearly in the characteristic mesh size h, while the total number of cells scales as h^2. This means that for even fairly coarse meshes the computation is quickly dominated by sweeping on the rectangular grid. This combined with the inaccuracy of homogenization makes the cut-cell method more accurate per unit computational cost.

4. Conclusions

The new linear cut-cell method shows significant promise. The method provides a relatively easy implementation of a second-order interface reconstruction technique that may be implemented in existing codes. The method has been shown to be significantly more accurate than homogenization in terms of the base orthogonal grid size as well as in terms of the total number of unknowns utilized. Additionally, there is evidence that the method is also substantially superior to homogenization in terms of accuracy per unit computational cost. Finally, it is worth noting that the method has the significant advantage of maintaining an underlying rectangular grid which greatly facilitates the use of a parallel solution algorithm.

REFERENCES

1. D. M. Ingram, D. M. Causon, C.G. Mingham, "Developments in Cartesian Cut Cell Methods", *Mathematics and Computers in Simulation*, **61**, pp.561-572 (2003).
2. J.E. Morel and G.R. Montry, "Analysis and Elimination of the Discrete-Ordinates Flux Dip," *Trans. Theory Stat. Phys.*, **13(5)**, pp. 615-633 (1984).